Journal Name

ARTICLE

Chiral Phosphoric Acid Catalysis: From Numbers to Insights

Rajat Maji,[a] Sharath Chandra Mallojjala,[a,b] and Steven. E. Wheeler[a,b]

Received 00th January 20xx,
Accepted 00th January 20xx

DOI: 10.1039/x0xx00000x

www.rsc.org/

Chiral phosphoric acids (CPAs) have emerged as powerful organocatalysts for asymmetric reactions, and applications of computational quantum chemistry have revealed important insights into the activity and selectivity of these catalysts. In this tutorial review, we provide an overview of computational tools at the disposal of computational organic chemists and demonstrate their application to a wide array of CPA catalysed reactions. Predictive models of the stereochemical outcome of these reactions are discussed along with specific examples of representative reactions and an outlook on remaining challenges in this area.

Key Learning points:

1. Quantitative and qualitative computational approaches that have been used to study CPA catalysed reactions.
2. Key stereocontrolling factors.
3. Overview of activation modes in CPA catalysis.
4. Proposed models to rationalise and predict stereochemical outcomes.
5. Important reaction types and key mechanistic insights driven by computation.

1. Introduction

Chiral phosphoric acid (CPA) catalysed reactions, interest in which has grown considerably over the last dozen years (see Figure 1A),[1] have opened up previously inaccessible enantioselective synthetic routes and now constitute a key area of growth in the field of organocatalysis. Despite this progress, considerable gaps in our understanding of the modes of activation and stereoinduction in these reactions remain. In recent years, computational studies have unravelled key aspects of these reactions, providing insight into their often high degrees of activity and stereoselectivity and paving the way for more effective CPA catalysed transformations.

Paton and co-workers[2] recently provided a tutorial review on the computational modelling of stereoselective organic reactions, covering both computational methods as well as fundamental concepts important for understanding stereoselectivity (kinetic vs. thermodynamic stereoselectivity, the Curtin-Hammett principle, *etc*). In this tutorial review, we build on this by delving more deeply into computational studies of CPA catalysed reactions in particular, showing how careful analyses of computed transition state (TS) structures can help turn numbers into insights. We commence with an outline of the computational tools that can be used to understand CPA catalysed reactions. Subsequently, we describe various factors impacting stereoselectivity followed by qualitative models that have been developed to predict the stereochemical outcomes of these reactions. Next, we discuss the primary activation modes operative in these reactions as well as important categories of CPA catalysed reactions in which computational studies have proved vital to understanding stereoselectivity. This is followed by examples in which computations have provided a deeper understanding of other mechanistic aspects of these reactions. We conclude by highlighting outstanding challenges and areas that deserve special attention. Although this review is focused primarily on CPAs, selected examples of similar axially chiral phosphoramidites and phosphoramides are also included, since computational chemistry has also provided important insights into these related transformations.

2. Theoretical Methods and Tools to analyse Reactions and the Stereoselectivity

2.1 Computational Methods

Quantum chemical methods applicable to large organic systems have matured considerably in recent years, and the relative free energies of transition states for complex organic reactions can be computed with remarkable accuracy. Such methods include combined quantum mechanics/molecular mechanics (QM/MM) and QM/QM methods as well as Kohn-Sham density functional theory (DFT), which is well-suited for systems with 50-100 atoms. In QM/MM-based methods, such as ONIOM, parts of the system are treated quantum

[a] Department of Chemistry, Texas A&M University, College Station, TX 77842 (USA)
[b] Center for Computational Quantum Chemistry, Department of Chemistry, University of Georgia, Athens, GA 30602 (USA)

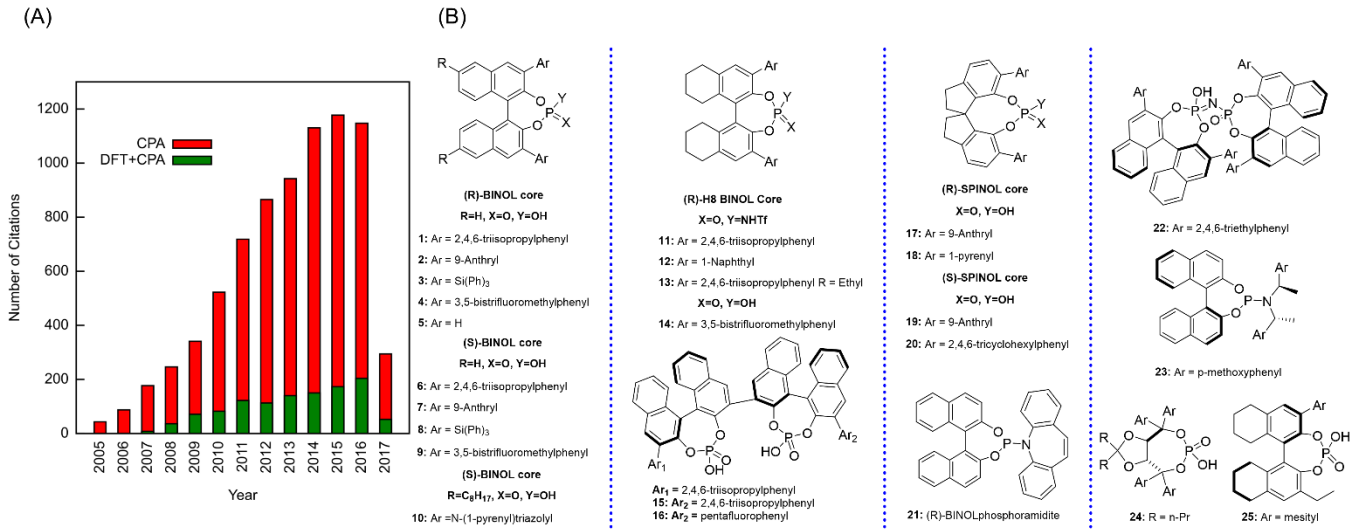

Figure 1. (A) Growth in the number of papers on CPA-catalysed reactions; (B) Chiral phosphoric acids (CPAs) and similar catalysts discussed in this work.

mechanically whereas other components (typically those not directly involved in the reaction) are treated using classical MM methods. A decade ago, such methods were widely employed to study CPA-catalysed reactions out of necessity. In these studies, the phosphoric acid moiety of the catalyst and the reactants were typically treated at the DFT level while the remaining components of the catalyst were treated at the MM level. However, with continued advances in computational hardware (following Moore's Law) and algorithms, reactions catalysed by large CPAs can now be treated entirely with DFT.

Such applications of DFT need to be done with care, however, to ensure that the many dispersion-driven noncovalent interactions operative in these systems (*vide infra*) are treated accurately. For example, the B3LYP functional, which for many years was the workhorse of computational organic chemistry, fails to account for dispersion-like interactions and can subsequently provide inaccurate results for CPA catalysed reactions. Luckily, the last decade has witnessed tremendous advancements in DFT methods that capture dispersion-driven interactions. Chief among these are the empirical dispersion corrections from Grimme *et al*. (the so-called –D methods), which can be coupled with any well-behaved DFT functional (B3LYP, B97, TPSS, *etc*.). The continuum solvent models PCM and SMD have proved sufficient (and necessary!) for many of these reactions, although inclusion of explicit solvent is sometimes required.

In general, stereoselectivity depends on the difference in free energy between competing transition states, $\Delta\Delta G^{\ddagger}$. However, we note that many authors utilize enthalpies (or even electronic energies) due to errors associated with computing the entropic contributions to $\Delta\Delta G^{\ddagger}$. Once structures of key TS structures have been optimized, the battle has only begun, and one must turn to other computational tools in order to understand the origin of the energy difference between stereocontrolling transition states. Such tools are described in the following sections.

2.2 Distortion-Interaction and Fragmentation Studies

Distortion-interaction analysis (or the activation-strain model), was introduced to explain trends in barrier heights of bimolecular reactions.[3] In such analyses, the reaction barrier ($\Delta E^{\ddagger}$) is decomposed into the energy required to distort the reactants into the TS geometry (ΔE_{dist}) and the interaction energy between these distorted fragments ($\Delta E_{int} = \Delta E^{\ddagger} - \Delta E_{dist}$). Distortion-interaction has also proved useful in explaining the difference in energy between stereocontrolling TS structures in asymmetric reactions. In such applications, the reaction barrier is decomposed into the energy required to distort the reacting substrates and catalyst into their TS geometries and the interaction energy between the distorted substrates and catalyst. It is important to note that in contrast to the original applications to bimolecular reactions, in which ΔE_{int} reflected the extent of formation of the forming/breaking bonds, in applications to asymmetric reactions ΔE_{int} reflects the noncovalent interactions between the substrate and catalyst; any differences in the extent of formation of forming/breaking bonds is included in the substrate distortion energy.

Distortion-interaction analyses can be complemented by fragmentation studies, in which selected portions of optimized TS structures (*e.g*. aryl-substituents) are removed and replaced with hydrogens while holding the rest of the structure fixed.[4,5] This can help pinpoint differences in interaction energies between similar stereocontrolling structures by systematically eliminating sources of noncovalent interactions. It should be noted, however, that such fragmentations often lead to only qualitative predictions of the strengths of these interactions; that is, the act of severing covalent bonds can lead to significant changes in the resulting interaction energies. The result is that the sum of individual interaction energies is not always in strict agreement with the interaction energies computed for the intact TS structures.

Within the framework of distortion-interaction analyses, the stereoselectivity of CPA-catalysed reactions can be distortion-controlled, interaction-controlled, or controlled by both distortion and interaction energies. Among distortion-

controlled reactions, stereoselectivity can arise from differences in either catalyst or substrate distortion, or both. For instance, Champagne and Houk[6] showed that distortion of the catalyst is mainly responsible for stereoselectivity in intermolecular oxetane ring-openings by *in situ* generated HCl (Scheme 1, reaction I). By excising the flanking aryl groups on the catalyst, they further showed that the excess catalyst distortion in TS_{minor} arises primarily from the phosphoric acid functionality of the catalyst. On the other hand, Duarte *et al*.[7] showed that in chiral phosphate mediated desymmetrizations of aziridinium and episulfonium ions (Scheme 1, reaction II), the stereoselectivity is primarily a result of excess substrate distortion in the TS leading to the minor stereoisomer.

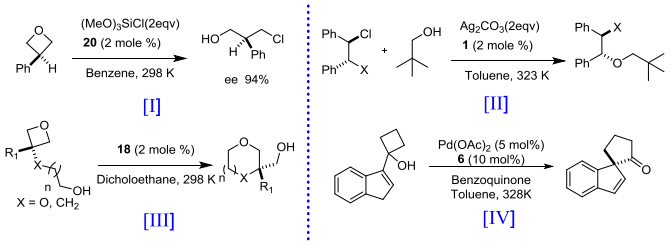

Scheme1.Reactions demonstrating the use of distortion-interaction analysis to explain stereoinduction.[5-8]

With regard to interaction-controlled reactions, Maji *et al*.[5] showed that the selectivity of reaction III (Scheme 1) is governed primarily by differences in interaction energies between the catalyst and substrates. Finally, Jindal *et al*.[8] provided a recent example in which both distortion and interactions control selectivity (Scheme 1, reaction IV). In this Pd(II)-Brønsted acid catalysed migratory ring expansion of an indenylcyclobutanol, DFT computed structures for the stereodetermining step exhibit a nearly orthogonal arrangement of two chiral phosphates around Pd in TS_{major}, while TS_{minor} shows a nearly coplanar arrangement. The square planer geometry around the Pd in the latter case leads to greater distortion than seen for TS_{major}. Furthermore, TS_{major} enjoys more C–H···π interactions compared to its counterpart and hence enjoys more favourable interactions.

Despite its demonstrated utility, distortion-interaction analyses alone do not always provide a comprehensive understanding of the mode of stereoinduction in CPA-catalysed reactions, since such analyses fail to quantify the separate contributions of steric interactions, dispersion interactions, and electrostatic interactions to the energy difference between stereocontrolling TSs.

2.3 AIM Analysis and NCI Plot

A number of computational tools have been developed to identify noncovalent interactions by analysing electron densities. In the atoms-in-molecules (AIM) framework, the presence of a bond path and bond critical point (BCP) along the bond path has been deemed an indicator of bonding interactions between two atoms. The stereoselectivity of several CPA-catalysed reactions has been attributed to differential noncovalent interaction based in part on the use of AIM to pinpoint crucial noncovalent contacts. For instance, Sunoj and co-workers[9,10] used AIM to identify the weak interactions responsible for stereoinduction in several CPA-catalysed reactions. In the case of an asymmetric sulfoxidation reaction,[9] preferential *Re* facial addition was explained by the greater number of favourable noncovalent contacts, as identified by AIM (Figure 2).

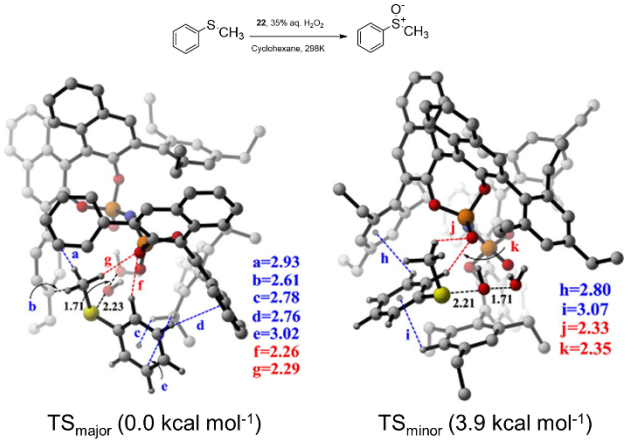

Figure 2. Stereocontrolling TS for CPA Catalysed asymmetric sulfoxidation reaction along with their relative free energies in kcal mol^{-1}.[9] Reprinted with permission from *Angew. Chem. Int. Ed.* 2014, **53**, 4432-4436.

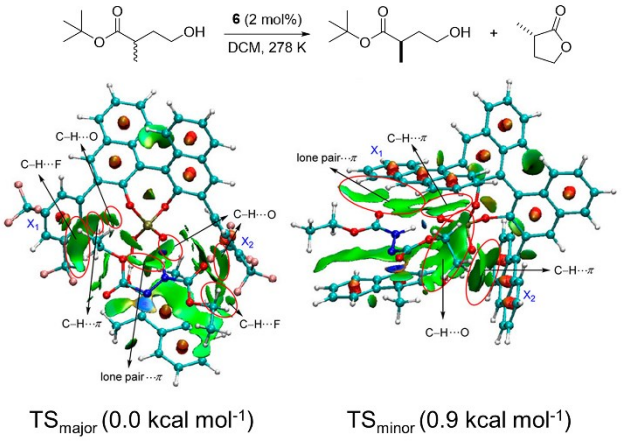

Figure 3. NCI analysis (blue, strong attraction; green, weak interaction; red, strong repulsion) of stereocontrolling TSs for CPA catalysed kinetic resolution of hydroxyl ester along with their relative free energies in kcal mol^{-1}.[11] Reprinted with permission from *Org. Lett.*, 2016, **18**, 3730-3733. Copyright 2016 American Chemical Society.

Noncovalent interactions can also be visualized by using the noncovalent interaction (NCI) index of Yang and co-workers,[12] which is also based on analyses of the electron density. Plots of the NCI index provide a qualitative mapping of inter- and intramolecular noncovalent interactions, with colours differentiating attractive and repulsive interactions. This enables a quick comparison of the dominant interactions operative in competing TSs. For instance, Changotra *et al*.[11] used NCI plots in their study of CPA catalysed kinetic resolutions of hydroxyl esters (Figure 3). Comparison of NCI plots for the major and minor TS structures reveals the presence of significantly more stabilizing dispersion-like interactions (green surfaces) in the former than in the latter.

2.4 NBO and Electrostatic Potentials (ESPs)

Finally, natural bond orbital (NBO) analyses and analyses of ESPs provide means of quantifying specific noncovalent

interactions in CPA-catalysed reactions. These approaches are particularly useful in unravelling the impact of competing noncovalent interactions in TS structures. For example, in their study of chiral phosphate mediated desymmetrizations (Scheme 1, reaction II), Duarte and Paton[7] utilised NBO second-order perturbation theory to quantify a key CH···O interaction between the catalyst and substrate (Figure 4A). Similarly, Paton and co-workers[13] also identified an important arene metal interaction in both the rate and stereodetermining oxidative coupling TS in the course of designing a chiral phosphoramadite ligand for a stereoselective Rh-catalysed [5+2] ynamide cycloaddition. In this case, NBO analysis enabled the quantification of π-d donation and d to π* back-bonding in this reaction (Figure 4B), providing key insights that formed the basis for the design of a modified ligand that provided enhanced selectivity.

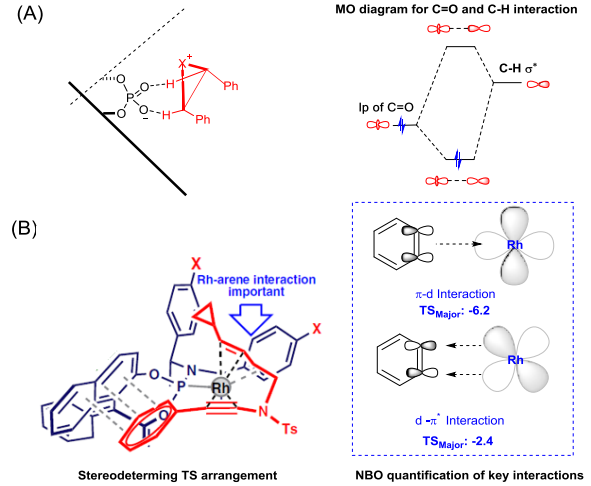

Figure 4: NBO quantification of interactions in CPA catalysis[7,13]

An estimate of electrostatic interactions can be gleaned from computed ESPs of stereocontrolling TSs. The ESP is the electrostatic interaction that a positive test charge would experience at a point in space near a molecule, and reflects the balance between the repulsion of this test charge by the nuclei and the attraction by the molecular electron density. Since the ESP at a given point depends on the electron density everywhere in space, even a remote change in the electron density distribution can impact the ESP at a given point. As such, one should be cautious not to conflate changes in the ESP with local changes in the electron density. In general, the electrostatic interaction between two molecules or molecular fragments can be approximated as the product of the charges due to one molecule (or fragment) with the ESP arising from the other molecule (or fragment). In this way, the electrostatic contributions of interactions in competing stereocontrolling TS structures can be compared in a semi-quantitative fashion. For example, Maji *et al*.[5] used ESPs to quantify the contribution of electrostatic interactions to the energy difference between stereocontrolling TS structures in intramolecular oxetane ring openings. They found that a key proton resides in a more favourable electrostatic environment in TS_{major} than in TS_{minor} (see Figure 5). More precisely, the ESP at the position of this in TS_{major} and TS_{minor} (Figure 5) is –122.3 and –108.1 kcal/mol, respectively. Taking the product of these ESPs with the corresponding NPA charges reveals a 3.0 kcal/mol preferential electrostatic stabilization of the former.

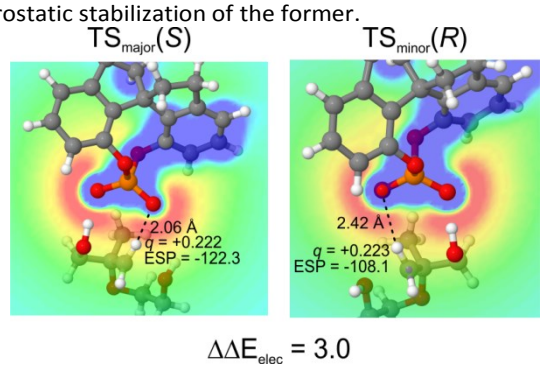

Figure 5. Quantification of relative electrostatic stabilization (ΔΔE, in kcal mol^{-1}) of a key proton in competing stereocontrolling TS structures.[5] The NPA charge (*e*) of this proton and ESP (in kcal/mol) due to the phosphate at the position of this proton are also provided. Modified with permission from *ACS Catal.*, 2017, **7**, 7332-7339. Copyright 2017 American Chemical Society.

3. Key Stereodetermining Factors in CPA Catalysed Reactions

3.1 Steric Environment

The steric environment around the chiral phosphoric acid framework has long been considered the dominant determining factor for stereoselectivity of CPA catalysed reactions. The presence of aryl side chains in the 3,3' positions of CPAs creates a well-defined, tunable chiral binding cavity for the reacting substrates. As such, many explanations of the stereoselectivity of CPA-catalysed reactions hinge on the destabilization of the disfavoured TS through steric interactions of the substrates with the flanking aryl groups of the catalyst. This is the basic presumption behind the "Quadrant Projection" and "Goodman Projection" models described below in Section 4.

Reid and Goodman[14] have championed the idea that steric interactions between substrates and CPA catalysts can be broadly divided into *proximal* and *remote* steric effects (Figure 6A). Moreover, they showed that these effects can be quantified based on readily computed energetic and geometric parameters of CPA catalyst components. In particular, proximal steric effects are captured by two physical parameters: 1) *A* values for the distal substituents, which correspond to the thermodynamic difference between diaxial and diequitorial conformations of 1,3-disubstituted cyclohexanes; and 2) rotational barriers of the aryl side chains, which capture the energy required for rotation around the central C-C bond to circumvent the destabilizing eclipsing interaction between attached R groups with the hydrogens of the opposing aryl ring. Remote steric interactions, on the other hand, can be described by the so-called AREA angle (A Remote Environmental Angle). AREA(θ) is defined as the smallest angle between the vector *p* (which goes from the midpoint of the naphthol oxygens to the Ph) and all possible *c* vectors (which extend from the Ph to each atom on the 3,3'-substituents).

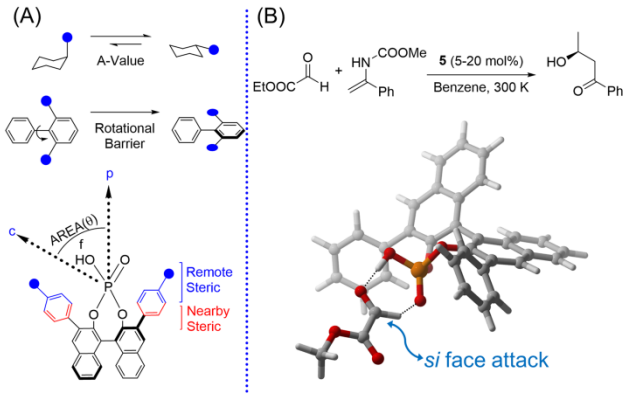

Figure 6. (A) Key steric parameters identified by Reid and Goodman[14] or CPA catalysed reactions. (B) Key stereocontrolling TS for a CPA-catalysed aza-ene reaction between glyoxylate and ene-carbamates.[15]

Steric interactions can impact stereoselectivity through two limiting mechanisms. Typically, these interactions destabilize one TS relative to competing TSs. In extreme cases, steric interactions can completely eliminate access to one prochiral face of a substrate in a pre-formed substrate/catalyst complex. The former category is widely represented in the examples of CPA-catalysed reactions discussed in Section 6. As far as the second group, Terada *et al.*[15] rationalised the enantioselectivity of a CPA-catalysed aza-ene reaction between glyoxylate and ene-carbamate based on DFT computations (see Figure 6B). They reported that the two H-bonds between the catalyst and glyoxolate in the pre-reaction complex forces a coplanar orientation of the substrate with the phosphoric acid moiety. Based on these results, they argued that the *re* face of the aldehyde is shielded by the aryl side chain of the catalyst, thereby promoting nucleophilic attack of the carbamate from the *si* face.

Steric interactions can be difficult to quantify, since frequently it is distortion effects that arise to avoid steric interactions that drive selectivity, not the steric interactions themselves. For instance, the confined size and shape of the binding cavity of CPAs often induces significant distortion of either the catalyst or substrates to avoid significant steric clashes; the two distortion-guided reactions[6,7] described in Section 2.2 are examples. This effect can be particularly pronounced for CPA's that are relatively rigid (*e.g.* SPINOL derived CPAs). The excellent performance of axially chiral imidodiphosphoric acids,[9] with respect to their monomeric counterparts, can also be attributed in part to the greater ability of these more confined binding pockets to discriminate between stereoisomers via steric effects.

3.2 Noncovalent Interactions

The last decade has seen an increasing appreciation of the importance of attractive noncovalent interactions in organic systems in general and CPA catalysed reactions in particular.[16,17] The presence of heteroatoms bearing significant partial charges as well as aryl groups that flank the reacting centre in CPAs can lead to myriad stabilizing noncovalent interactions in the stereocontrolling TSs. These interactions include π-stacking, CH···π, C=O···H, C-H···O, and lone-pair···π interactions, among others. Recent advances in our understanding of these interactions have enabled their use as key design elements CPA-catalysed reactions.[16]

Recently-reported reactions from the Toste and Sigman groups[16] demonstrate the power of noncovalent interactions to dictate the stereochemical outcome of CPA-catalysed reactions. For instance, they showed[16] that a stacking interaction between a triazole on the catalyst and an aryl component of the substrate was pivotal in an enantioselective oxidative amination (Scheme 2, reaction I). They also demonstrated[16] an enantiodivergent fluorination of allylic alcohols that exploits lone-pair···π interactions (Scheme 2, reaction II).

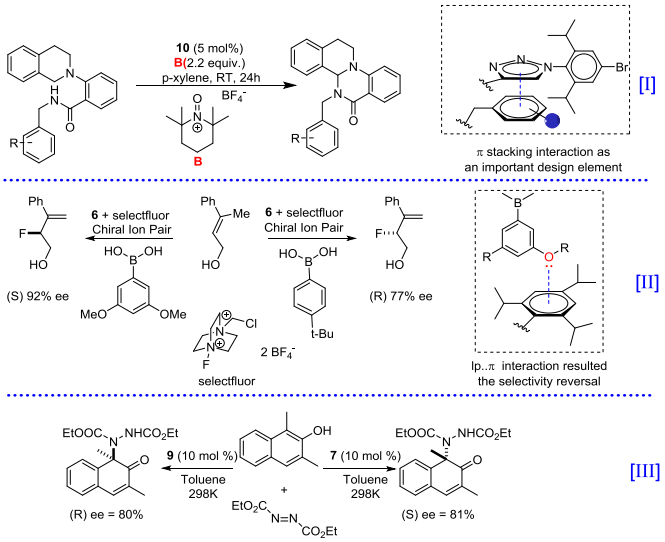

Scheme 2: Exploitation of noncovalent interaction to design new stereoselective reaction.[16] CPA dependent stereo reversal in asymmetric dearomative amination of β-naphthols.[18]

Noncovalent interactions can also lead to reversal of selectivity. For example, Changotra *et al.*[18] demonstrated the potential for noncovalent interactions to dictate the stereochemical outcome of an asymmetric dearomative amination of β-naphthols (Scheme 2, reaction III). In this case, changing the aryl substituent on the CPA from 3,5-$(CF_3)_2$-C_6H_3 (**4**) to 9-anthryl (**2**) lead to a reversal in selectivity. This was explained in terms of the change in preferred orientation of the substrate within catalyst cavity. With **4**, the substrates were positioned perpendicular to the 3,3' substituents while with **2** they adopt a nearly parallel orientation. This, in turn, changed the pattern of noncovalent interactions from predominantly C–H···F to C–H···π in the stereocontrolling transition states, leading to the observed stereoreversal.

Often, the role of attractive noncovalent interactions in stereoinduction is obvious when examining the competing TS structures; a strongly stabilizing interaction might be present in the preferred TS but completely absent in the disfavoured TS. For instance, Tambar and co-workers[19] documented the role of noncovalent interactions in the enantioselectivity of a CPA catalysed aza-Claisen rearrangement (Figure 7A). Through computations, they showed that the catalyst engages with the substrate via NH···O and CH···O interactions; the 9-anthracenyl

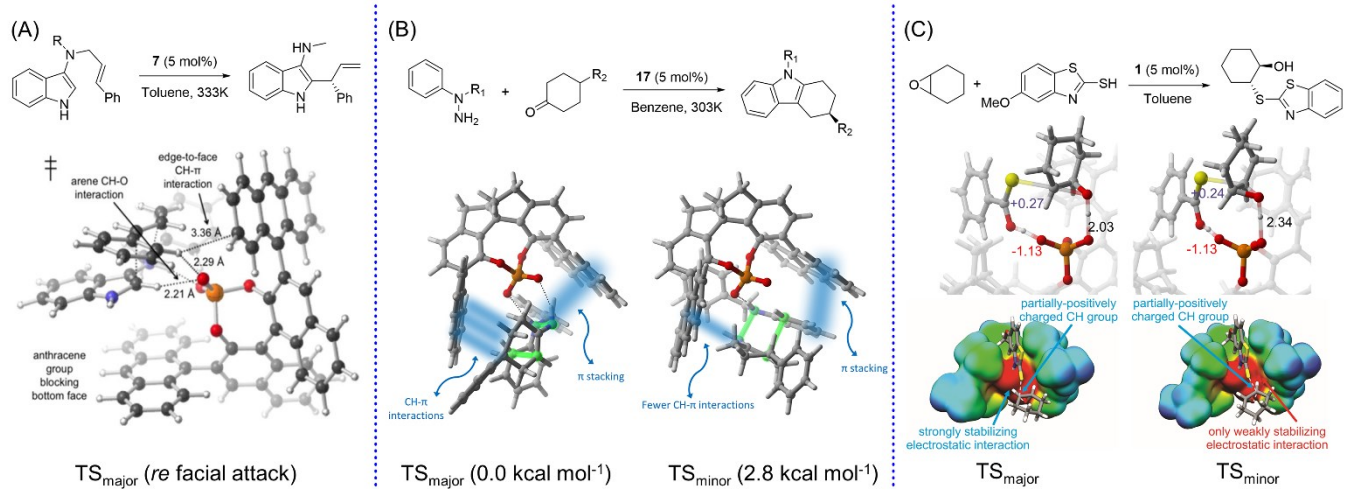

Figure 7. (A) CPA-catalysed aza-Claisen rearrangement.[19] Modified with permission from *J. Am. Chem. Soc.*, 2013, **135**, 16380-16383. Copyright 2013 American Chemical Society (B) DFT computed stereodetermining TSs of CPA-catalysed Fischer Indolization along with the free energies in kcal mol^{-1}.[20] (C) CPA-catalysed intermolecular epoxide openings. Modified with permission from *ACS Catal.*, 2016, **6**, 2681-2688.[4] Copyright 2016 American Chemical Society.

group of the catalyst then blocks the bottom *si* face, forcing the reaction to take place on the less crowded *re* face. Moreover, it was shown that the higher selectivity in the case of aromatic substituents, compared to aliphatic ones, can be attributed to stabilizing edge-to-face CH···π interactions in the former case.

However, in some cases the role of noncovalent interactions in stereoinduction is less clear, since many competing attractive interactions can be present in both the major and minor TSs. In such cases, one must quantify the individual interactions to pinpoint those primarily responsible for preferential stabilization of the favoured TS. For instance, Seguin and Wheeler[20] recently studied the CPA catalysed Fischer indole reaction in Figure 7B, identifying the two lowest lying TSs for the stereocontrolling [3,3]-sigmatropic rearrangement. TS$_{major}$ was found to be 2.8 kcal/mol lower in free energy than TS$_{minor}$, providing reasonable agreement with the observed selectivity. Distortion-interaction analysis of these TS structures provided an interaction energy difference of 4.8 kcal/mol, which was partitioned into contributions from different noncovalent interactions via fragmentation. It was observed that while H-bonding interactions favour TS$_{major}$, π-stacking interactions between the substrate and anthryl groups favour the minor TS. The dominant factor in this reaction turned out to be CH···π interactions, which favour the major TS by an overwhelming 5 kcal/mol.

A relatively unexplored property of CPA catalysts is their ability to achieve stereodifferentiation by constraining the orientation of the reacting substrates within the highly heterogeneous electrostatic environment of the binding cavity and thereby preferentially stabilizing one transition state over others. Often, CPAs protonate the substrate, and the subsequent TS structures correspond to ion-pairs. In many cases, the 3,3'-aryl groups of the CPA create a narrow cleft that restricts the orientation of the reacting substrates within the chiral electrostatic environment of the depronated catalyst. This can result in the preferential electrostatic stabilization of fleeting or permanent partial charges in the reacting substrates. Given the strength of electrostatic interactions compared to dispersion-driven interactions, for example, even small differences in the orientation of the substrate between two competing TS structures can have a substantial impact on enantioselectivity. Seguin *et al*.[4] and Maji *et al*.[5] have noted such examples in the context of CPA-catalysed epoxide and oxetane ring-openings, respectively. In both cases, examination of the ESPs of the competing TS structures proved informative (see Figure 7C), as did quantifying the electrostatic stabilization of key C-H groups in these structures (as described in Section 2.4). In the case of the asymmetric ring-opening of epoxides (Figure 7C), the TS structure leading to the preferred isomer is preferentially stabilized by electrostatic interactions of the C-H undergoing nucleophilic attack (which bears a significant partial positive charge during the TS) by the phosphoryl oxygen of the deprotonated catalyst.[4] This electrostatic mode of stabilization in epoxide ring openings gained further support from a later study by List *et al*.[21]

3.3 Phosphoric Acid pK$_a$

The judicious tuning of catalyst acidity has also proved fruitful as a path to catalyst optimization. For instance, Houk *et al*.[22] observed that the acidity of the Brønsted acid catalyst is crucial for the efficiency of (3^+ + 2) cycloadditions of hydrazones with alkenes; lower acidic phosphoric acids are ineffective, while more acidic chiral *N*-triflylphosphoramides proved highly selective. They analysed[22] these reactions using DFT, showing that the superior performance of *N*-triflylphosphoramidite based catalysts over CPAs can be attributed to distortion effects. That is, because of the higher acidity of the phosphoramidite, the cycloaddition TS requires little distortion of the ion pair complex. The inability of CPAs to protonate the hydrazones leads to greater distortion to achieve the TS geometry. Similarly, dithio-analogues of CPAs, whose pK$_a$'s are generally lower than the corresponding CPAs,

have proved effective in a number of transformations. In general, both yield and selectivity often suffer when these various acid catalysts with pK_a's outside of an ideal window for a given reaction are used.

Despite significant progress, a proper physical organic basis behind such pK_a-dependence remains elusive. One way to understand these effects would be to determine the acidity of these CPAs and correlate these with reactivity. However, the difficulty of experimentally determining reliable pK_a's of these catalysts hinders such studies. Gratifyingly, recent theoretical work by Cheng *et al*.[23,24] has provided DFT-based predictions of pK_a's for CPA catalysts in DMSO to a precision of ~0.4 pK_a units, offering a possible route to more definitive studies of structure-activity relationship and rational tuning of CPA-like catalysts. Moreover, this computational approach is applicable to CPAs in presence of other catalysts, opening the door to tuning the CPA pK_a's in the context of cooperative catalysis.

4. Models to Predict Stereochemical Outcomes

A primary aim of many computational studies is the development of a general, predictive model of the stereochemical outcome of reactions. One of the earliest such models was the Quadrant Projection of Himo[25] and Terada,[26] which has formed the foundation for explanations of a wide array of CPA-catalysed reactions. In Quadrant Projection, the catalyst is viewed along the C_2-axis (Figure 8), resulting in the aryl substituents on the catalyst occupying two of four 'quadrants'. The preferred TS structure is generally the one in which the substrates are positioned in the unoccupied quadrants, providing a simple visual tool for a qualitative understanding of stereoselectivity. This quadrant model was modified by Goodman *et al*.,[27] and has been used to develop a general predictive model of imine hydrogenation reactions. In the so-called Goodman Projection (Figure 8), the catalyst is oriented such that the BINOL oxygens are in the plane of the page, leaving the phosphoryl group lying above and below the page along with the aryl substituents. This provides an alternative visualization of steric interactions between the substrates and catalyst. These quadrant models have formed the basis for more specific predictive models of the stereochemical outcome of particular reactions. Representative examples are discussed below.

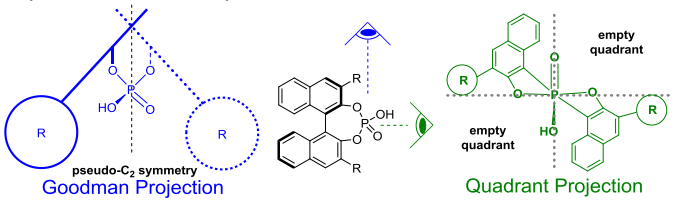

Figure 8. Goodman Projection and Quadrant projection of a CPA catalyst.[25,27]

It is important to recognize that increasing steric demand does not always translate into greater selectivity; instead, it can stop the reaction altogether or even reverse the sense of stereoinduction. One case, from Reid and Goodman,[14] involves the transfer hydrogenation of an imine (Figure 9), in which reversal of stereoselectivity is observed depending on the size of the 3,3'-substituents. Reid and Goodman[14] proposed a model, based on their remote and proximal steric parameters (Figure 6), that can be used to predict the outcome of this complex CPA catalysed transformations. In this reaction, the imine can be oriented in two different ways with respect to the 3,3' groups (Type 1 and Type 2). Moreover, the imine can be in either a cis (Z) or trans (E) conformation based on internal steric demand, leading to four unique TS arrangements for such reactions (two of which are shown in Figure 9). Among these, Type 1E and Type 2Z furnish the (S)-product while Type 1Z and Type 2E afford the (R)-product. ONIOM computations indicate that for catalysts **6** and **8**, Type 1 is preferred. However, these computations also show that Type 1Z is preferred with catalyst **6** but Type 1E is preferred with **8**. This was explained in terms of the strikingly different steric parameters for these two catalysts. For **8**, the catalyst cavity is of a medium size, and the E conformation is preferred over Z in order to reduce internal steric interactions in the imine. For **6**, on the other hand, the larger 3,3'-groups result in a much smaller catalyst cavity and the steric interactions between the R groups and the aryl side chains outweigh the energetic cost of internal steric repulsions. The result is a preference for Type 1Z and a reversal of stereoselectivity compared to **8**.

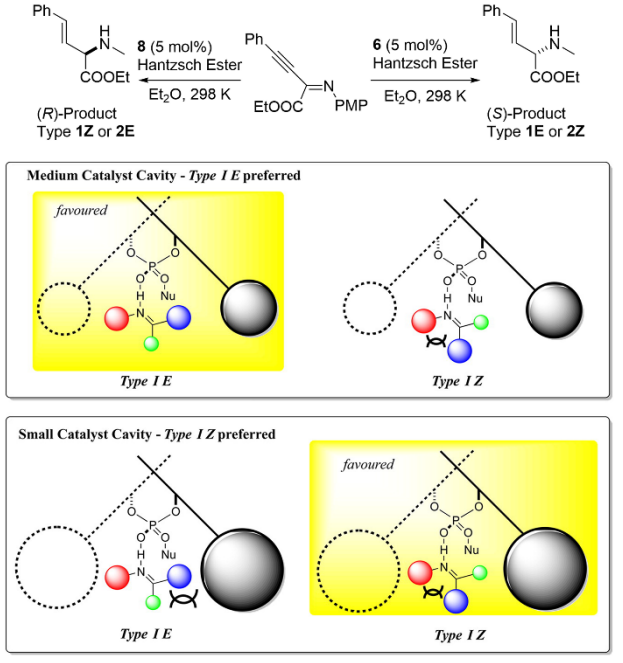

Figure 9. Model to account for proximal and distal steric requirements in bifunctional CPA-catalysed reactions of imines.[28] Reprinted with permission from *Acc. Chem. Res.*, 2016, **49**, 1029-1041. Copyright 2016 American Chemical Society.

Goodman *et al*.[29] and Houk and co-workers[30] have both studied CPA catalysed allylation and propargylation reactions, showing that these reactions proceed via cyclic, six membered chair-like transition states. Two distinct TS models have been proposed to explain the selectivity (see Figure 10). In both models, the Brønsted acidic functionality of the CPA activates

the boronate ester through a hydrogen bond. While the pseudo-equatorial oxygen of the boronate is activated in Houk's model, the pseudo-axial oxygen of the boronate is activated in Goodman's model. Furthermore, in Goodman's model the formyl hydrogen interacts with the Lewis basic part of the CPA, while in Houk's model electrostatic interactions are responsible for orienting the aldehyde. Further studies showed that transition states corresponding to these two models are of comparable energy for formation of the major isomer, indicating that both models are potentially relevant to formation of this stereoisomer. However, Houk's model was found to be the dominant pathway for formation of the minor isomer. While steric interactions are primarily responsible for the stereoselectivity in Goodman's model, stereoselectivity in Houk's model is due to distortion of the catalyst to avoid steric interactions.

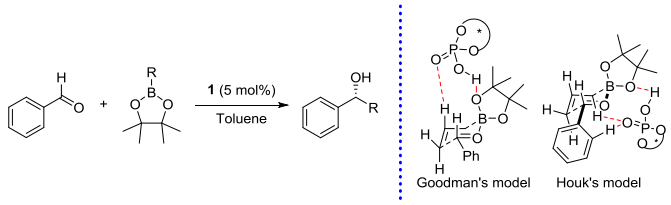

Figure 10.CPA catalysed allylation and propargylation of aldehydes.[29]

Champagne and Houk[6] proposed a working model for intermolecular oxetane openings (Scheme 1, reaction I) based on Quadrant Projection.[6] According to their model (Figure 11), the nucleophile and the leaving group occupy the empty quadrants in TSs leading to both the major and minor products, which projects the larger substituent of the oxetane *anti* to the catalyst. From this projection, one can predict the preferred isomer considering the overall steric interaction. The TS that would suffer minimum steric repulsion between the substituent of the oxetane (blue sphere) and the substituents at the para position of the catalyst walls (black spheres) is predicted to be favoured. This simple model is remarkably successful at predicting the stereochemical outcome for other intermolecular oxetane openings and amination reactions without any further computations.

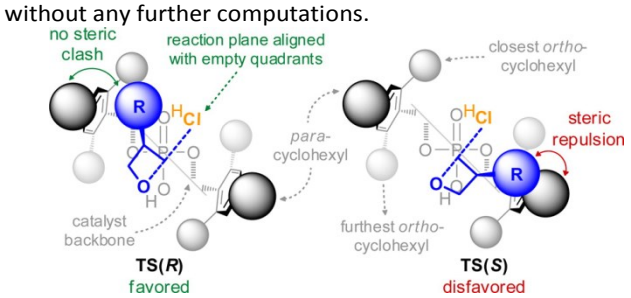

Figure 11. Stereochemical model to predict the outcome of an intermolecular oxetane openings .[6] Reprinted with permission from *Journal of the American Chemical Society*, 2016, **138**, 12356-12359. Copyright 2016 American Chemical Society.

Despite the success of this model, it failed to explain the outcome of intramolecular oxetane desymmetrizations. In light of this, Maji *et al.*[5] recently proposed two new models (Figure 12) that explain the stereoselectivity of these reactions. The difference is that in these intramolecular reactions, the coordination of both the electrophile and nucleophile with the acid and basic sites of the CPA requires significant substrate distortion. The result is a qualitatively different activation mode in these intramolecular reactions (see below) and a qualitatively different origin of selectivity. Moreover, the presence or absence of a chelating group (*e.g* OH) leads to qualitatively different TS arrangements than seen for substrates without chelating groups.

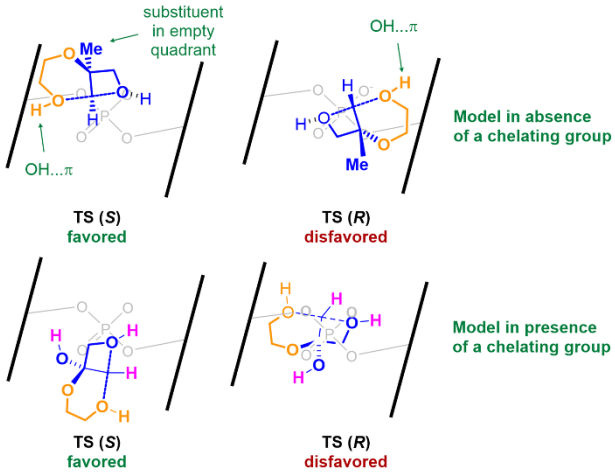

Figure 12. Two different models for intramolecular oxetane opening.[5] Reused with permission from *ACS Catal.*, 2017, **7**, 7332-7339. Copyright 2017 American Chemical Society.

5. Overview of Binding and Activation Modes

Understanding the binding and activation mode is vital for designing new CPA catalysed reactions. In conventional CPA-catalysed reactions, activation occurs by the lowering of the LUMO energy of the substrate through either hydrogen bonding or protonation by the phosphoric acid. This has traditionally been thought to occur via two primary modes, dual activation and bifunctional (either inter- or intramolecular) activation (Figure 13A).

However, computations have revealed additional activation and binding modes, broadening the scope of CPA catalysed reactions. For example, while CPA activation typically involves two-point contact (which is generally thought to impart greater selectivity), Calleja *et al.*[31] showed the feasibility of one point coordination in the context of an asymmetric Povarov reaction (Figure 13B). DFT computations indicated the favourability of an atypical one point coordination between the imine and the chiral phosphoric acid that maximizes π-stacking interactions while minimizing steric interactions in the transition state. In a similar spirit, Maji *et al.*[5] recently reported (Figure 13C) a distortion-guided activation mode in the case of intramolecular oxetane openings (Scheme 1, reaction III). In the preferred TS, the phosphoric acid activates the oxetane through an OH···O hydrogen bonding interaction while the aryl substituent of the catalyst activates the nucleophilic oxygen via an OH···π interaction. This "oxetane activation" mode was shown to be more favourable than more conventional activation modes, which can be understood in terms of the relative

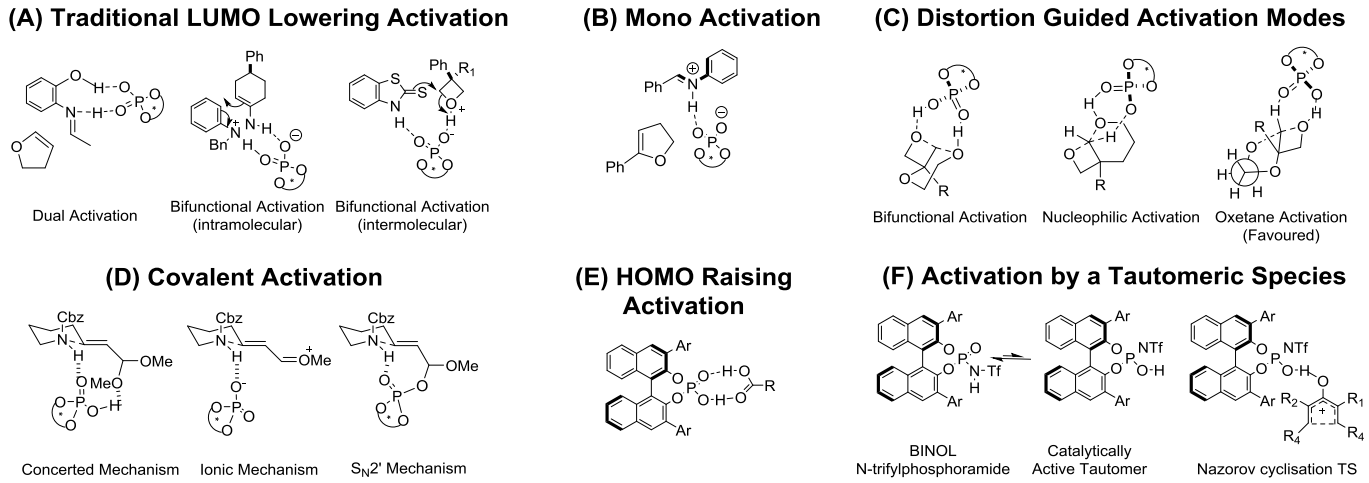

Figure 13. Various activation modes in CPA catalysis identified through computational studies.

distortion energies of the substrates in the corresponding TS structures. For the traditional bifunctional activation mode, the substrate distortion is substantial due to the ring strain required to engage in two OH···O interactions with the catalyst. This strain is largely alleviated in oxetane activation, in which one OH···O interaction is replaced with a CH···O interaction. The lack of distortion in this mode more than compensates for the relative weakness of the CH···O interaction compared to an OH···O hydrogen bond.

While CPA catalysis typically occurs via noncovalent activation of the substrates, computations have also identified examples of covalent activation. This is somewhat unexpected, as the formation of covalent bonds typically leads to the deactivation of CPA-based catalysts. However, Nagorny, *et al*.[32] studied the CPA catalysed synthesis of piperidines through an intramolecular cyclization of unsaturated acetals. They showed that an unexpected SN2′ pathway is favoured over the expected concerted or ionic mechanisms (Figure 13D).

Recent computational and experimental work from Thiel, List, *et al*.[21] has revealed that CPAs can also activate substrates by raising the HOMO energy. In contrast to the more common LUMO lowering pathway, computed FMO energies reveal that the HOMO energy of acetic acid is increased upon complexation with TRIP while the energy of the LUMO remains almost unchanged (Figure 13E). This represents a potentially powerful new mode of activation for CPA catalysed reactions.

New binding modes of chiral phosphoramides have also been identified through computations. While the active form of chiral phosphoramides is typically thought to be the more stable amide tautomer (*i.e*. NHX and P═O),[22] Krenske and co-workers[33] showed that the active form of a BINOL-*N*-triflylphosphoramide catalysed enantioselective Nazarov cyclization is the less-stable tautomer containing a P(═NTf)OH group (Figure 13F). This was attributed to the more facile protonation of the substrate from an OH compared to NH, which occurs concomitantly with ring closure. Interconversion between tautomers was predicted to be fast, relative to electrocyclization, making this process viable under Curtin-Hammett conditions.

6. Reactions involving Phosphoric Acids

Having discussed computational tools, qualitative models, and the major activation modes operative in CPA catalysis, we now turn to representative examples of CPA catalysed transformations that have been analysed computationally. Stereoselective CPA catalysed reactions can generally be grouped into five categories: Brønsted acid catalysis, chiral counterion catalysis, chiral anion phase transfer catalysis, chiral cooperative catalysis, and chiral relay catalysis. While the literature on CPA catalysis is dominated by Brønsted-acid mediated reactions, computational studies have also been applied to these other categories. Below, we mainly focus on Brønsted-acid mediated catalysis (Sec. 6.1), followed by a more abbreviated discussion of other modes (Sec. 6.2).

6.1 Brønsted-acid Catalysis

6.1.1 Asymmetric Hydrogenations

DFT has been applied to a number of CPA-catalysed hydrogenations. For example, Simón and Goodman[34] studied a Hantzsch ester mediated hydrogenation, revealing that the bifunctional activation mode is preferred. Based on this bifunctional activation, the selectivity of this reaction was explained in terms of a three-point model based on steric interactions. In the case of acyclic imines, E-Z interconversion is rapid and the reaction proceeds through the Z-conformer to avoid steric interactions between the incoming nucleophile and the catalyst. This model is supported by analyses of the Goodman Projection of the computed TS structures. Phenylimine forms a complex with the phosphoric acid through hydrogen bonding, leaving the bulky substituents oriented away from the 3,3′-substituents of the catalyst. The Brønsted acid functionality of the catalyst then activates the nucleophile, completing the three-point contact model. Because they cannot freely interconvert between *E* and *Z* conformations, the stereochemistry in the case of cyclic imines is dictated by the stereochemistry of the imine in order to minimize steric interactions (Figure 14).

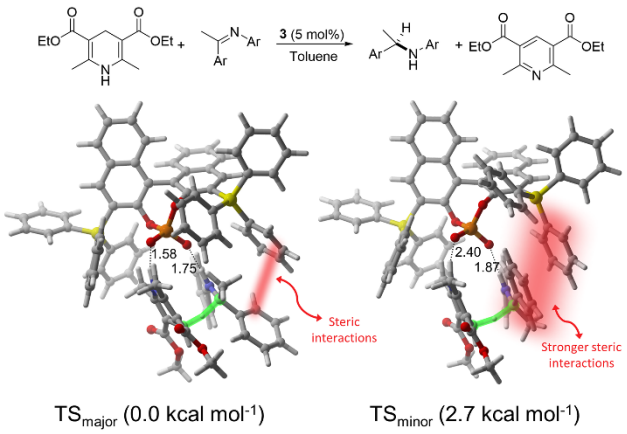

Figure 14. Stereodetermining TSs of CPA catalysed Hantzsch ester mediated hydrogenation along with their free energies in kcal mol^{-1}.[34]

6.1.2 Kinetic Resolutions and Dynamic Kinetic Resolution

Akiyama *et al*.[35] utilized CPA-catalysed transfer hydrogenation for the oxidative kinetic resolution of indolines. DFT studies suggested a cyclic TS in which the Brønsted acidic proton activates the ketimine while the Lewis basic phosphoryl oxygen hydrogen bonds with the indoline N-H, thus activating both substrates. Examining the Quadrant Projection suggests that the *syn* ketimine is favoured over the *anti* ketimine due to steric factors (Figure 15), explaining the observed stereoselectivity.

Nimmagadda *et al*.[36] recently reported the synthesis of chiral oxime ethers via the dynamic kinetic resolution (DKR) of cyclohexanones catalysed by metal salts of CPAs. Computed structures for the stereocontrolling transition states revealed shape complementarity between the reacting substrates and chiral binding pocket of the catalyst in the case of the TS leading to the major stereoisomer. This resulted in more favourable NH···O and CH···π interactions in this TS, which lead to the observed stereoselectivity (Figure 16).

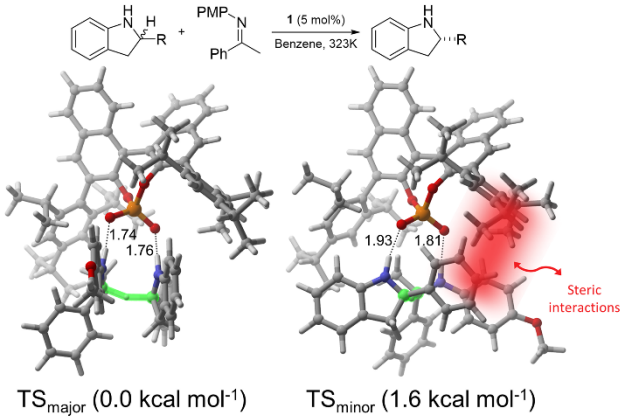

Figure 15. TS showing key interactions in the oxidative kinetic resolution of indolines along with their relative electronic energies in kcal mol^{-1}.[35]

6.1.3 Desymmetrizations

Intramolecular and intermolecular desymmetrizations of epoxides and oxetanes have been studied computationally by a number of groups.[5,6,21,37,38] Some aspects of these reactions have already been discussed in the sections above; below, we briefly summarize key findings along with two other desymmetrization reactions. Ajitha and Huang[37] first studied the asymmetric ring-opening of *meso* epoxides using DFT. They reported that the reaction proceeds via a concerted bifunctional pathway where a C-H···O interaction combined with steric effects govern the enantioselectivity. Subsequently, Seguin and Wheeler[4] performed a more extensive study of nine reactions/catalyst combinations, arriving at a slightly different understanding of these reactions (Figure 7C). They argued that the difference in CH···O distance observed by Ajitha and Huang[37] is a consequence of other noncovalent interactions, and does not account for the free energy difference between the stereocontrolling TSs. Instead, they explained the preferential nucleophilic attack of one carbon over the other to the different electrostatic environments of the two carbons of the epoxide within the heterogenous electrostatic environment of the deprotonated catalyst. This resulted in the preferential electrostatic stabilization of a transient positive charge in the major TS, which ultimately gave rise to the observed stereoselectivity.

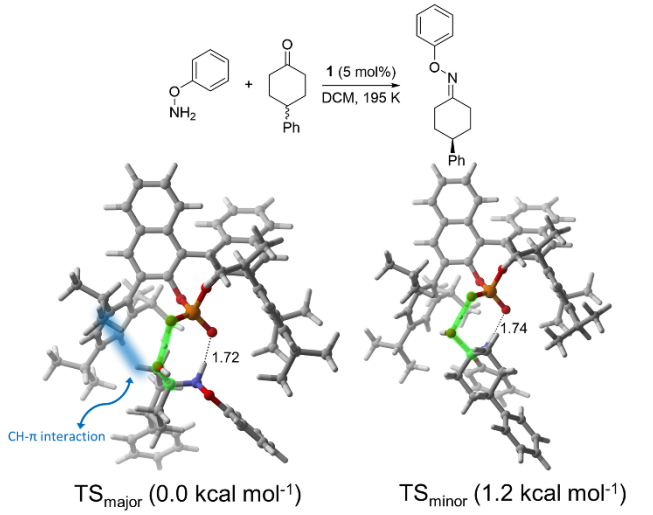

Figure 16. DFT optimized TS structures leading to the favoured and disfavoured stereoisomeric oxime ethers along with relative free energies in kcal mol^{-1}.[36]

Seguin and Wheeler[38] and Champagne and Houk[6] independently studied the catalytic enantioselective intermolecular desymmetrizations of oxetanes, arriving at disparate conclusions regarding the origin of selectivity. Champagne and Houk[6] pinpointed catalyst distortion as the primary contributor to selectivity in intermolecular oxetane desymmetrizations by HCl, proposing a general model for stereoinduction in such reactions. On the other hand, Seguin and Wheeler[38] examined four examples of oxetane ring openings by mercaptobenzothaizoles (see a representative example in Figure 17), showing that the mode of stereoinduction and TS structures changed markedly with small variation in substrate and catalyst. Overall, they reported that stereoselectivity is governed by the interplay of many relatively modest noncovalent interactions, precluding the development of a general stereochemical model. Similarly, Maji *et al*.[5] recently showed that the stereoselectivity of intramolecular oxetane desymmetrization (Scheme 1, reaction

III) is controlled primarily by competing electrostatic and π-stacking interactions. Unlike the epoxide desymmetrizations studied by Seguin and Wheeler,[4] the impact of electrostatic interactions in these oxetane desymmetrizations depends on nature of the chelating group.

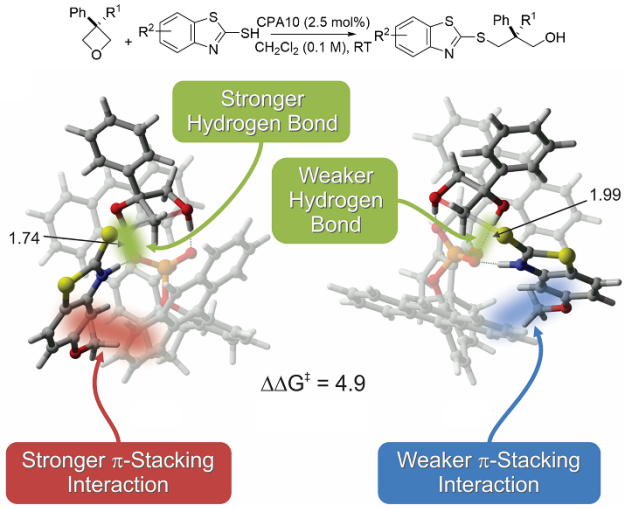

Figure 17. Intramolecular oxetane openings by marcaptobenzothiazoles,[38] in which the left structures leads to the major product. (Relative free energies in kcal mol^{-1}) Modified with permission from *ACS Catal.*, 2016, **6**, 7222-7228. Copyright 2016 American Chemical Society.

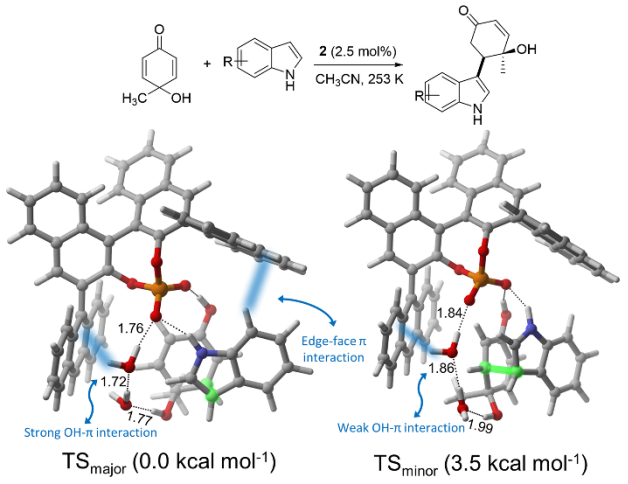

Figure 18. TSs showing major interactions involved in CPA catalysed FC alkylation along with their computed free energies in kcal mol^{-1}.[39]

Garcia *et al.*[39] studied the desymmetrization of cyclohexadiones via a Fridel-Crafts alkylation experimentally (Figure 18), finding that the exclusion of water from the reaction decreased both the rate and enantioselectivity. DFT computations provided a compelling explanation for this intriguing experimental outcome. First, the experimental data could be reproduced only if two explicit water molecules were included in the computations. The associated TS structures revealed two important roles of water. First, the presence of water results in a more compact catalyst cavity in the major TS. Second, water preferentially stabilizes the major TS by engaging in an OH···π interaction with the anthracenyl substituent on the catalyst. TS_{major} is further stabilized by an edge-to-face aryl-aryl interaction between the indole and the other anthracenyl group (Figure 18).

Houk *et al.*[40] studied the CPA catalysed oxidative desymmetrization of substituted diols via oxidative cleavage of benzylidineacetals (Figure 19). To explore the origin of enantioselectivity, the authors used a model biphenol-derived CPA to study the key proton-transfer TS. The computed free energy of TS_{major} was 2.0 kcal/mol lower than that of TS_{minor}, in good agreement with the 95% *ee* obtained experimentally. Given the lack of obvious steric interactions in these two competing TS structures, the authors argued that stereodifferentiation arises from the orientation of the *p*-methoxyphenyl (PMP) group of the substrate relative to the bulky aryl substituent on the catalyst. While these two aryl groups are distant in the minor TS, they engage in a stabilizing T-shaped interaction in TS_{major}. This aryl–aryl interaction was shown to contribute the majority of the energetic preference for TS_{major}. Given the importance of this interaction, the authors predicted that replacement of the PMP group in the original substrate with methyl would significantly erode the enantioselectivity. This was validated experimentally.

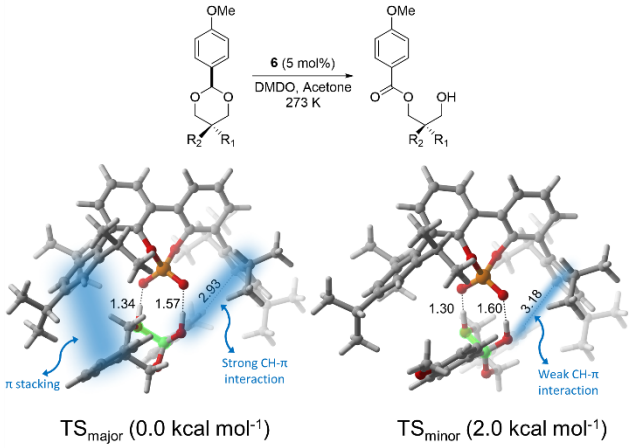

Figure 19. Stereodetermining TSs for oxidative desymmetrization of benzylidineacetals, along with their relative free energies in kcal mol^{-1}.[40]

6.1.4 Pericyclic Reactions

Bis-phosphoric acids have been shown to be more acidic than monophosphoric acids, and can form extensive hydrogen bonding networks. Terada *et al.*[41] exploited these features to develop bis-phosphoric acid based catalysts (**21** and **22** in Figure 1), demonstrating their efficacy in an asymmetric Diels-Alder cycloaddition (Figure 20). Computations suggest that the (*S, R, S*) atropodiasteriomer of the symmetric catalyst (**21**) is favoured and the chiral environment provided by this catalyst is distinct from that of the corresponding CPA due to the hydrogen bonding network. Steric interactions between the substrates and the aryl substituent on the catalyst were pinpointed as the source of stereoselectivity. The impact of electron withdrawing groups on one of the aryl substituents was investigated by considering the C_1-symmetric CPA catalyst **22**. Computed TS structures showed that the introduction of this electron-deficient aryl group perturbs the chiral reacting space by altering the pK_a of the adjacent phosphoric acid

proton. This example not only demonstrates the use of computations to probe electronic effects and noncovalent interactions in CPA catalysis, but also demonstrates the importance of properly tuning pK_a in CPA catalysed reactions.

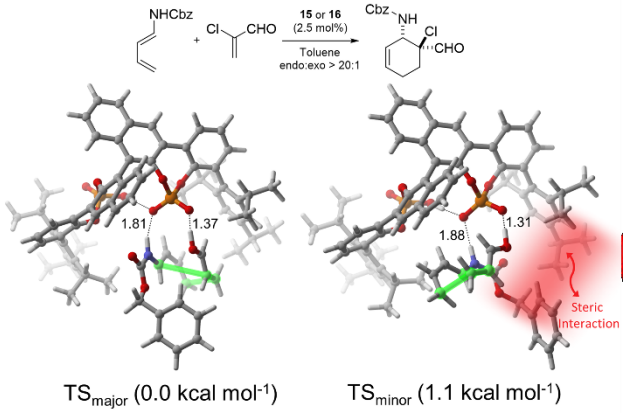

Figure 20. C_2-symmetric bis-phosphoric acid catalysed Diels Alder reaction from Terada and co-worker's along with their free energies in kcal mol^{-1}.[41]

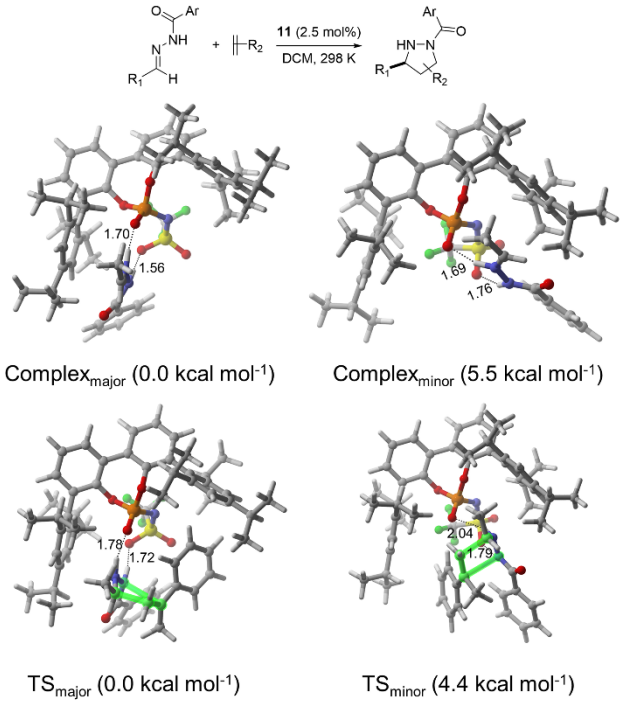

Figure 21. DFT optimized ion pair complexes and stereodetermining TSs of *N*-Triflylphosphoramide catlaysed (3^+ + 2) cycloaddition along with their free energies in kcal mol^{-1}.[22]

Houk and co-workers[22] addressed several issues related to *N*-triflylphosphoramide catalysed (3^+ + 2) cycloadditions between hydrazine and alkenes (Figure 21), including the preferred protonation state and reaction pathway, the origin of stereoinduction, and the relatively poor selectivity in the case of ethyl vinyl thioethers. Initial protonation of the hydrazone by the *N*-triflylphosphoramide produces an ion pair that subsequently undergoes a (3^+ + 2) cycloaddition with the alkene. This is preferred over the alternative (3 + 2) cycloaddition involving the analogous azomethine imine due to greater stability of the hydrazine compared to the azomethine imine. The origin of enantioselectivity was ascribed to the steric demand of the bulky substituents of the catalyst, which leaves only one pro-chiral face of the hydrazonium available for alkene approach. Consistent with this model, the low enantioselectivity of ethyl vinyl thioethers, compared to α-methyl styrene, can be explained by its smaller size; the large binding pocket of [H8]-BINOL-based triflylphosphoramide does not provide the same high degree of enantioselectivity as in the case of α-methyl styrene.

The importance of electronic effects in CPA-catalysed pericyclic reactions was demonstrated by Kürti *et al.*[42] in their enantioselective BINAM synthesis. They ascribed the stereoselectivity in the key [3,3]-sigmatropic shift transition states to both steric and electronic effects (Figure 22). The chiral counterion creates an asymmetric binding pocket for the protonated substrate. In addition, the electron-withdrawing CF_3 groups of the catalyst lead to enhanced CH···π and π–stacking interactions that favour TS_{major}. Consistent with this model, replacing the CF3 groups in this catalyst with Me resulted in decreased stereoselectivity.

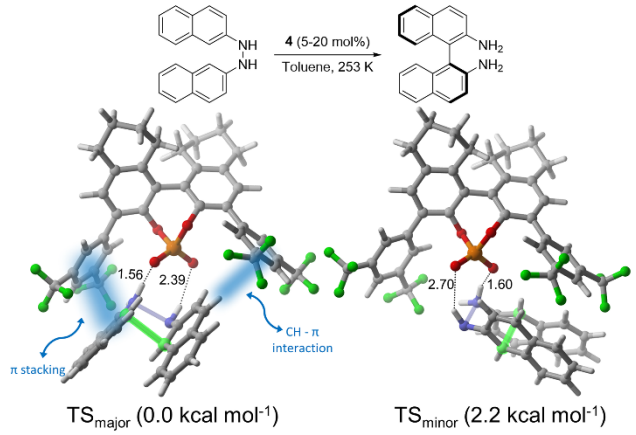

Figure 22. DFT-optimized CPA catalysed TSs of [3,3] sigmatropic rearrangement of *N,N'*-diaryl hydrazines along with their free energies in kcal mol^{-1} from Kürti *et al.*[42]

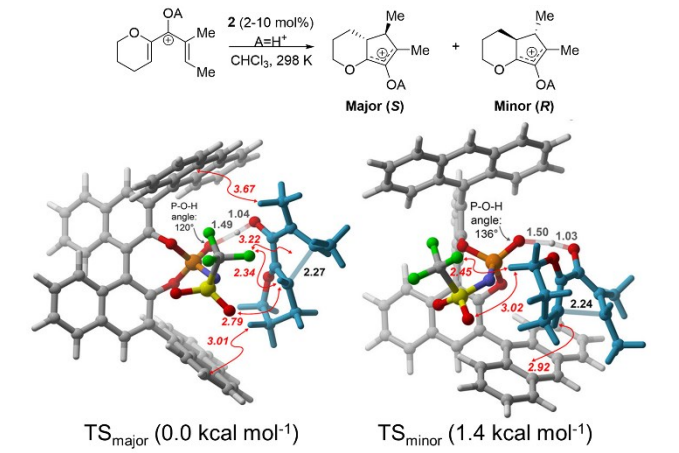

Figure 23. DFT-optimized TSs of chiral phosphonamide catalysed Nazarov cyclization of dihydropyranyl vinyl ketones with relative free energies in kcal mol^{-1}.[33] Reprinted with permission from *ACS Catal.*, 2017, **7**, 3466-3476. Copyright 2017 American Chemical Society.

Krenske and co-workers[33] recently reported on the enantioselectivities of Nazarov cyclizations of three classes of divinylketones by chiral phosphoramide based catalysts. They

found that the selectivity is dependent on a combination of factors, including catalyst distortion, the degree of proton transfer, intramolecular substrate stabilization, and a wide range of intermolecular noncovalent interactions (CH···π, cation–π, CH···O, CH···F, and cation–lone pair interactions) between the substrate and catalyst in the transition state. All of these interactions depended on a tight fit of the cyclizing divinyl ketone into the chiral binding pocket of the catalyst, and the selectivity was attributed to the greater catalyst distortion in TS_{minor} due to widening of the P-O-H angle in order to accommodate the substrate within the catalyst cavity (Figure 23).

6.2 Alternative Modes of Catalysis

There are a number of other modes of catalysis open to CPAs and related catalysts. For instance, the ability of these catalysts to work cooperatively with other catalysts has garnered significant interest in the last decade; computational studies can provide key insights that aid the development of such complex catalytic systems. Several examples in this area have recently been highlighted by Sunoj and co-workers[43] so here we present two new examples where phosphoric acid or phosphoramide based catalysts work cooperatively to achieve high selectivity, as well as other novel modes of CPA catalysis.

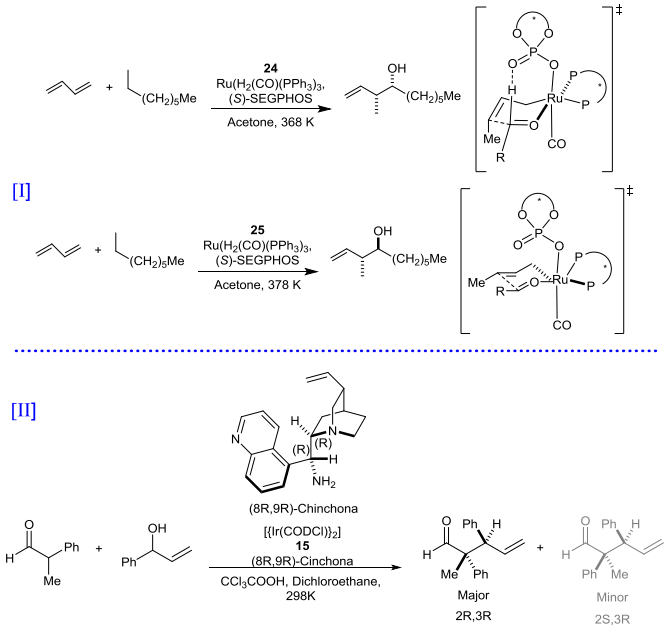

Scheme 3. Stereodivergence in hydroxy alkylation of butadienes using cooperative catalysis (reaction I)[44] and cooperative dual catalytic asymmetric α-allylation (reaction II).[10]

Grayson *et al.*[44] studied Ru and CPA cooperativity in the context of the asymmetric hydroxyalkylation of butadienes (Scheme 3, reaction I). Based on DFT computations, they reasoned that the chiral phosphate dependent steroselectivity results from a CH···O interaction between the phosphoryl oxygen and the formyl proton of the aldehyde in the case of TADDOL derived catalysts. With this favourable CH···O interaction in place, the *syn* selectivity can be understood by the preferential reaction of (Z)-s-crotylruthenium with aldehydes in which the crotyl methyl group is placed in a pseudo-axial position to alleviate *gauche* interactions with the aldehyde. On the contrary, for BINOL-derived catalysts this CH···O interaction is not present, since its formation would lead to a steric clash between the chiral phosphine and the chiral phosphate ligand. Consequently, with these catalysts nucleophilic attack occurs on the opposite prochiral face of the aldehyde, leading to *anti* selectivity.

Bhaskararao and Sunoj[10] studied the stereodivergence in an asymmetric α–allylation reaction under the cooperative action of a chiral Ir-phosphoramidite and cinchona amine (Scheme 3, reaction II). One intriguing aspect of this reaction is the ability to alter the chirality of each stereocentre of the product by employing the enantiomer of the corresponding catalyst. For instance, when the (*R*,*R*)-cinchona is used with (*R*)-phosphoramidite, the major product has a (2*R*,3*R*) configuration at the the α and β–centres. These configurations can be inverted simply by using the (*S*,*S*)-cinchona and (*S*)-phosphoramidite. Computational analysis indicates that the configuration of the β carbon is determined during the formation of an Ir-π-allyl intermediate. Consistent with experiment, the lowest energy TS leading to the (2*R*,3*R*) product involves *re* facial addition of (*R*,*R*)-cinchona-enamine to the *si* face of the Ir-(R)-phosphoramidite intermediate. Transition states corresponding to *si-si* and *si-re* additions were significantly higher in energy, which is consistent with the experimentally observed high enantio- and diastereoselectivity. These energy differences were attributed to the preferential stabilization of one TS through π-stacking and CH···π interactions.

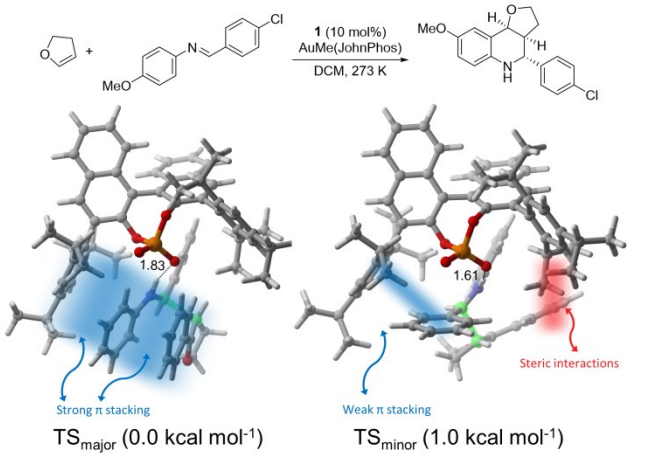

Figure 24. Stereodetermining TSs for the three component orthogonal relay catalysis along with the relative free energies in kcal mol^{-1}.[31]

Rodriguez and co-workers[31] recently highlighted the importance of π-stacking and steric interactions in Au and CPA mediated orthogonal relay catalysis in the enantioselective synthesis of hexahydrofuro[3,2-c] quinolones via a Pavarov reaction. The authors showed that the reaction follows a stepwise pathway rather than the commonly assumed concerted pathway. Computations further showed that the TS leading to the major *exo* product is stabilized by π-stacking interactions while also minimizing steric interactions (Figure 24). The reduced selectivity in toluene was attributed to the

destabilization of a key π–π–π interaction in TS_{major} due to competitive stacking interactions with the solvent.

Jindal and Sunoj[45] studied a multicatalytic allylation reaction, showing that the chiral phosphate serves as a counterion rather than a ligand for Pd. In particular, they demonstrated that Pd-bis-phosphine was the active species and, due to its larger volume, the chiral phosphoric acid can only interact as a counterion. Consequently, chirality transfer takes place through an outer sphere effect.

Finally, Paton and co-workers[7] recently performed the first theoretical study of asymmetric chiral anion phase transfer (CAPT) catalysis for *meso* aziridinium and episulfonium ring openings using both QM and Molecular dynamics (MD) simulations. Their study offers valuable insights into ion-pairing, ring-opening, and catalyst deactivation pathways. Explicitly solvated classical MD simulations and QM computations were used to explore possible ion-pairing geometries and to compute reliable interaction energies. Their results showed that the formation and stability of the ion pair is dramatically reduced with increased solvent polarity. TS computations further indicated that the stereoselectivity of the ring opening is mainly controlled by distortion of the substrate. Computed pathways for catalyst deactivation showed that under normal stoichiometric condition catalyst deactivation can be competitive with ring opening, thereby necessitated the use of excess alcohol.

7. Other Mechanistic Insights

Computational chemistry has also provided mechanistic insights into CPA catalysis beyond stereoselectivity. For instance, computations have been used to identify and explain preferred reaction pathways, to identify the nature of intermediates among several possibilities, and to uncover new, unexpected pathways.

For example, Jindal and Sunoj46 found that ligand exchange was critical to determine the low-energy pathway for a Pd(II))-Brønsted acid catalysed migratory asymmetric ring expansion of an indenylcyclobutanol to a spirocyclic indane. Of the two mechanistic possibilities examined, a Wacker-type pathway (involving a semi-pinacol ring expansion followed by reductive elimination) was found to be energetically favoured over the alternative allylic pathway (in which ring expansion of a Pd-π allyl intermediate occurs after the initial allylic C-H activation). Computations further indicated that the replacement of the native acetate ligands on Pd by phosphate and water stabilized a crucial TS structure. Remarkably, the authors showed that a phosphate mediated C-H activation pathway is more favourable than the widely accepted acetate-assisted activation. The phosphoric acid was shown to play a dual role in this process; during the first step, it is bound to the Pd as a ligand, lowering the energy, while in the second step it remains in the outer sphere and relays the indenyl β-proton to the Pd bound phosphate.

Similarly, Paton *et al*.[13] studied two potential mechanisms for a Rh-catalysed stereoselective [5+2]-cycloisomerization of ynamide vinyl cyclopropanes. In contrast to previous studies, their computations supported a revised mechanistic sequence in which an irreversible, stereodetermining C-C coupling between the reactants takes place before the metal insertion into the vinyl cyclopropane.

Thiel and co-workers[47] offered a revised view of the Brønsted acid-catalysed cyclization of an α,β-unsaturated hydrazine. Although this reaction had previously been classified as a 6π electrocyclization, computations suggest a non-pericyclic nature. In view of the computational results, they argued that this reaction can either be classified as a pseudo-pericyclic reaction or a 5 *endo*-polar mechanism in which the lone pair of nitrogen attacks the allylic group.

MD simulations have also provided key insights into the dynamics of CPA catalysed reactions. For instance, Houk *et al*.[48] used MD simulations to characterize C-H···O interactions in CPA catalysed allylborations, corroborating their previous model (Figure 10). In the gas phase, they showed that there is a significant enhancement of C-H···O and O-H···O interactions moving from the reactant to the TS; this effect is present but much weaker in toluene due to solvent caging. This was attributed to the build-up of partial charge during the transition state due to the forming B···O bond. This charge separation leads to an increase in the acidity of the benzaldehyde H and basicity of the allylboronate oxygen, which in turn enhances the C-H···O and O-H···O interactions in the TS relative to reactants and products. Finally, Zimmerman and co-workers[49] recently used MD simulations to probe the potential of a short-lived oxocarbenium intermediate along the concerted path in a (6,6)-spiroketalization. MD trajectories starting at the concerted TS structure revealed a short overall reaction time, which is consistent with a concerted asynchronous mechanism that avoids this oxocarbenium intermediate. These MD trajectories also indicated that alcohol deprotonation and ring closure occur simultaneously.

8. Future Directions

As documented above, our understanding of CPA catalysed reactions has witnessed tremendous growth over the last decade, driven in part by computational studies. Despite these advancements, some aspects of these reactions remain relatively unexplored and we wish to point out a few areas where computational studies can provide a foundation for future development.

First, modern quantum chemistry can aid in the design of reactions that are still relatively underdeveloped. For instance, it has been observed that highly reactive electrophiles are incompatible with CPA catalysis, presumably due to background decomposition pathways in which the catalyst is engaged in an undesired nucleophilic attack to form an inactive alkylated species. List *et al*.[21] recently circumvented this problem in the CPA-catalysed conversion of epoxides to thiiranes through the formation of a heterodimer that prevents catalyst deactivation. Computational studies can potentially generalize this approach to other, related systems.

On the other hand, reactions of inert substrates (*e.g.* C-H functionalization, or activation of inert C-C bonds) still pose a formidable challenge in CPA catalysed reactions, representing an area in which computations can play a leading role. Although there have been promising examples of cooperative catalysts in recent years, there is still a lack of mechanistic understanding of these transformations. Rigorous computational analyses of such reactions are likely to pave the way for further developments. Along these lines, the predictions of pK_a's of CPA catalysts from Cheng *et al*.,[23,24] either as an independent catalysts or in presence of another catalyst, could prove fruitful in the development of new reactions.

Secondly, a proper understanding of stereodetermining TS structures can facilitate the *de novo* design of CPA catalysts. Sunoj and co-workers[50] provided a pioneering example of the power of such design efforts in which they predicted stereoselectivities for new catalysts for an asymmetric diamination reaction. Going a step further, Anderson *et al*.[13] recently demonstrated the computationally-guided improvement of selectivity in enantio- and diastereoselective ynamide [5+2] cycloisomerizations. Our hope is that continued developments will open up the doors for the more routine use of computational chemistry in the design of CPA-based catalysts.

Finally, recent studies have shown that stereoselectivity sometimes arises from the complex interplay of a number of factors. Often in such cases, application of conventional computational tools alone is insufficient to untangle the many contributing factors. Sigman and co-workers[51] have demonstrated the power of combining experimental and computational data through the identification of multi-parameter linear free energy relationships as a means of identifying the many factors that impact stereoselectivity in complex CPA catalysed reactions. Such studies represent the forefront of combined experimental/computational studies of CPA-catalysed reactions.

9. Conclusions

Computational chemistry has made enormous strides in the last few years explaining the origin of activity and selectivity of CPA catalysed reactions, which in turn can inform the design of new reactions. We hope this tutorial review will not only provide an overview of the methods and techniques at the disposal of the computational organic chemist, but will also help guide both synthetic chemists and budding computational organic chemists hoping to make maximal use of computational data in research into CPA catalysed reactions. Together, this will aid future studies of chiral phosphoric acid catalysed reactions.

Acknowledgements

This work was supported by National Science Foundation (Grant CHE-1665407).

Notes and references

1 D. Parmar, E. Sugiono, S. Raja and M. Rueping, *Chem. Rev.*, 2014, **114**, 9047-9153.
2 Q. Peng, F. Duarte and R. S. Paton, *Chem. Soc. Rev.*, 2016, **45**, 6093-6107.
3 F. M. Bickelhaupt and K. N. Houk, *Angew. Chem. Int. Ed.*, 2017, **56**, 10070-10086.
4 T. J. Seguin and S. E. Wheeler, *ACS Catal.*, 2016, **6**, 2681-2688.
5 R. Maji, P. A. Champagne, K. N. Houk and S. E. Wheeler, *ACS Catal.*, 2017, **7**, 7332-7339.
6 P. A. Champagne and K. N. Houk, *J. Am. Chem. Soc.*, 2016, **138**, 12356-12359.
7 F. Duarte and R. S. Paton, *J. Am. Chem. Soc.*, 2017, **139**, 8886-8896.
8 G. Jindal and R. B. Sunoj, *Org. Lett.*, 2015, **17**, 2874-2877.
9 G. Jindal and R. B. Sunoj, *Angew. Chem. Int. Ed.*, 2014, **53**, 4432-4436.
10 B. Bhaskararao and R. B. Sunoj, *J. Am. Chem. Soc.*, 2015, **137**, 15712-15722.
11 A. Changotra and R. B. Sunoj, *Org. Lett.*, 2016, **18**, 3730-3733.
12 E. R. Johnson, S. Keinan, P. Mori-Sánchez, J. Contreras-García, A. J. Cohen and W. Yang, *J. Am. Chem. Soc.*, 2010, **132**, 6498-6506.
13 R. N. Straker, Q. Peng, A. Mekareeya, R. S. Paton and E. A. Anderson, *Nat. Commun.*, 2016, **7**, 10109.
14 J. P. Reid and J. M. Goodman, *J. Am. Chem. Soc.*, 2016, **138**, 7910-7917.
15 M. Terada, K. Soga and N. Momiyama, *Angew. Chem. Int. Ed.*, 2008, **47**, 4122-4125.
16 F. D. Toste, M. S. Sigman and S. J. Miller, *Acc. Chem. Res.*, 2017, **50**, 609-615.
17 R. B. Sunoj, *Acc. Chem. Res.*, 2016, **49**, 1019-1028.
18 A. Changotra, S. Das and R. B. Sunoj, *Org. Lett.*, 2017, **19**, 2354-2357.
19 P. Maity, R. P. Pemberton, D. J. Tantillo and U. K. Tambar, *J. Am. Chem. Soc.*, 2013, **135**, 16380-16383.
20 T. J. Seguin, T. Lu and S. E. Wheeler, *Org. Lett.*, 2015, **17**, 3066-3069.
21 M. R. Monaco, D. Fazzi, N. Tsuji, M. Leutzsch, S. Liao, W. Thiel and B. List, *J. Am. Chem. Soc.*, 2016, **138**, 14740-14749.
22 X. Hong, H. B. Küçük, M. S. Maji, Y.-F. Yang, M. Rueping and K. N. Houk, *J. Am. Chem. Soc.*, 2014, **136**, 13769-13780.
23 C. Yang, X.-S. Xue, J.-L. Jin, X. Li and J.-P. Cheng, *The Journal of Organic Chemistry*, 2013, **78**, 7076-7085.
24 C. Yang, X.-S. Xue, X. Li and J.-P. Cheng, *The Journal of Organic Chemistry*, 2014, **79**, 4340-4351.
25 T. Marcelli, P. Hammar and F. Himo, *Chem. Eur. J.*, 2008, **14**, 8562-8571.
26 I. D. Gridnev, M. Kouchi, K. Sorimachi and M. Terada, *Tetrahedron Lett.*, 2007, **48**, 497-500.
27 L. Simón and J. M. Goodman, *The Journal of Organic Chemistry*, 2011, **76**, 1775-1788.
28 J. P. Reid, L. Simón and J. M. Goodman, *Acc. Chem. Res.*, 2016, **49**, 1029-1041.
29 M. N. Grayson, S. C. Pellegrinet and J. M. Goodman, *J. Am. Chem. Soc.*, 2012, **134**, 2716-2722.
30 H. Wang, P. Jain, J. C. Antilla and K. N. Houk, *The Journal of Organic Chemistry*, 2013, **78**, 1208-1215.
31 J. Calleja, A. B. Gonzalez-Perez, A. R. de Lera, R. Alvarez, F. J. Fananas and F. Rodriguez, *Chem. Sci.*, 2014, **5**, 996-1007.

32 Z. Sun, G. A. Winschel, P. M. Zimmerman and P. Nagorny, *Angew. Chem. Int. Ed.*, 2014, **53**, 11194-11198.
33 J. P. Lovie-Toon, C. M. Tram, B. L. Flynn and E. H. Krenske, *ACS Catal.*, 2017, **7**, 3466-3476.
34 L. Simón and J. M. Goodman, *J. Am. Chem. Soc.*, 2008, **130**, 8741-8747.
35 K. Saito, Y. Shibata, M. Yamanaka and T. Akiyama, *J. Am. Chem. Soc.*, 2013, **135**, 11740-11743.
36 S. K. Nimmagadda, S. C. Mallojjala, L. Woztas, S. E. Wheeler and J. C. Antilla, *Angew. Chem. Int. Ed.*, 2017, **56**, 2454-2458.
37 M. J. Ajitha and K.-W. Huang, *Org. Biomol. Chem.*, 2015, **13**, 10981-10985.
38 T. J. Seguin and S. E. Wheeler, *ACS Catal.*, 2016, **6**, 7222-7228.
39 C. García-García, L. Ortiz-Rojano, S. Álvarez, R. Álvarez, M. Ribagorda and M. C. Carreño, *Org. Lett.*, 2016, **18**, 2224-2227.
40 S.-S. Meng, Y. Liang, K.-S. Cao, L. Zou, X.-B. Lin, H. Yang, K. N. Houk and W.-H. Zheng, *J. Am. Chem. Soc.*, 2014, **136**, 12249-12252.
41 N. Momiyama, K. Funayama, H. Noda, M. Yamanaka, N. Akasaka, S. Ishida, T. Iwamoto and M. Terada, *ACS Catal.*, 2016, **6**, 949-956.
42 G.-Q. Li, H. Gao, C. Keene, M. Devonas, D. H. Ess and L. Kürti, *J. Am. Chem. Soc.*, 2013, **135**, 7414-7417.
43 G. Jindal, H. K. Kisan and R. B. Sunoj, *ACS Catal.*, 2015, **5**, 480-503.
44 M. N. Grayson, M. J. Krische and K. N. Houk, *J. Am. Chem. Soc.*, 2015, **137**, 8838-8850.
45 G. Jindal and R. B. Sunoj, *The Journal of Organic Chemistry*, 2014, **79**, 7600-7606.
46 G. Jindal and R. B. Sunoj, *J. Am. Chem. Soc.*, 2014, **136**, 15998-16008.
47 B. Heggen, M. Patil and W. Thiel, *J. Comput. Chem.*, 2016, **37**, 280-285.
48 M. N. Grayson, Z. Yang and K. N. Houk, *J. Am. Chem. Soc.*, 2017, **139**, 7717-7720.
49 Y. Y. Khomutnyk, A. J. Argüelles, G. A. Winschel, Z. Sun, P. M. Zimmerman and P. Nagorny, *J. Am. Chem. Soc.*, 2016, **138**, 444-456.
50 G. Jindal and R. B. Sunoj, *Org. Biomol. Chem.*, 2014, **12**, 2745-2753.
51 M. Orlandi, F. D. Toste and M. S. Sigman, *Angew. Chem. Int. Ed.*, 2017, **56**, 14080-14084.

Biographies

Rajat Maji grew up in West Bengal, India and obtained his M.S. degree from IIT-Kharagpur working on the synthesis of modified carbohydrates under the tutelage of Tanmaya Pathak. He spent one year as a CSIR Junior Research Fellow working with Saumen Hajra on asymmetric organocatalysis. After joining Texas A&M as a grad student in 2012, he spent time in the Burgess Group working on the design of small molecules to perturb protein-protein interactions before joining the Wheeler Group in 2014.

SharathChandra Mallojjala grew up in Hyderabad, India. He obtained his undergraduate degree in the sciences from IISER-Pune in 2015 with an emphasis on Chemistry and Physics, where his research was focussed on the synthesis of natural product analogues and medicinal chemistry. He joined the Wheeler Group at Texas A&M in the Fall of 2015 and subsequently transferred to the Center for Computational Quantum Chemistry (CCQC) at the University of Georgia (UGA) in 2017. His current research interests include understanding organocatalysed and metal-catalysed reactions.

Steven E. Wheeler graduated from New College of Florida with a B.A. in Chemistry and Physics and completed his Ph.D. working with Fritz Schaefer at the CCQC at UGA in 2006. He was an NIH NRSA Postdoctoral Fellow in Ken Houk's group at UCLA before joining the faculty at Texas A&M in 2010. He was promoted to Associate Professor with tenure in 2015 and named Davidson Professor of Science in 2016. He moved to his present position at UGA in January, 2017. His group works in the area of computational physical organic chemistry studying the role of noncovalent interactions in organocatalysis, organic electronic materials, and drug design.

TOC Figure